AD-A061 161 ARMY ELECTRONICS RESEARCH AND DEVELOPMENT COMMAND FO--ETC F/G 17/6
VARIABLE TEMPERATURE MULTIMODE MAGNETOMETER.(U)
SEP 78 J J WINTER, F ROTHWARF, H A LEUPOLD

UNCLASSIFIED DELET-TR-78-21 NL

| OF |
AD
A061 161

END
DATE
FILMED
1-79
DDC

[redacted]

12 B.S.

9 RESEARCH AND DEVELOPMENT TECHNICAL REPORT,

14 DELET-TR-78-21

6 VARIABLE TEMPERATURE MULTIMODE MAGNETOMETER,

10 J. J./Winter,
F./Rothwarf,
H. A./Leupold
J. T./Breslin

ELECTRONICS TECHNOLOGY & DEVICES LABORATORY

11 September 1978 12 9 p.

16 1L161102AH47

DISTRIBUTION STATEMENT

Approved for public release;
distribution unlimited.

17 E7

ERADCOM

US ARMY ELECTRONICS RESEARCH & DEVELOPMENT COMMAND
FORT MONMOUTH, NEW JERSEY 07703

NOTICES

Disclaimers

The citation of trade names and names of manufacturers in this report is not to be construed as official Government indorsement or approval of commercial products or services referenced herein.

Disposition

Destroy this report when it is no longer needed. Do not return it to the originator.

UNCLASSIFIED
SECURITY CLASSIFICATION OF THIS PAGE (When Data Entered)

REPORT DOCUMENTATION PAGE		READ INSTRUCTIONS BEFORE COMPLETING FORM
1. REPORT NUMBER DELET-TR-78-21	2. GOVT ACCESSION NO.	3. RECIPIENT'S CATALOG NUMBER
4. TITLE (and Subtitle) VARIABLE TEMPERATURE MULTIMODE MAGNETOMETER		5. TYPE OF REPORT & PERIOD COVERED 6. PERFORMING ORG. REPORT NUMBER
7. AUTHOR(s) J.J. Winter H.A. Leupold F. Rothwarf J.T. Breslin		8. CONTRACT OR GRANT NUMBER(s)
9. PERFORMING ORGANIZATION NAME AND ADDRESS Electronic Materials Research Division US Army Electronics Technology & Devices Laboratory (ERADCOM) Fort Monmouth, NJ 07703 DELET-ES		10. PROGRAM ELEMENT, PROJECT, TASK AREA & WORK UNIT NUMBERS 61102A 1L161102AH47 E7 031
11. CONTROLLING OFFICE NAME AND ADDRESS US Army Electronics Research & Development Command Fort Monmouth, NJ 07703 DELET-ES		12. REPORT DATE September 1978 13. NUMBER OF PAGES 5
14. MONITORING AGENCY NAME & ADDRESS(if different from Controlling Office)		15. SECURITY CLASS. (of this report) Unclassified 15a. DECLASSIFICATION/DOWNGRADING SCHEDULE

16. DISTRIBUTION STATEMENT (of this Report)

Approved for public release; distribution unlimited.

17. DISTRIBUTION STATEMENT (of the abstract entered in Block 20, if different from Report)

18. SUPPLEMENTARY NOTES

This paper was published in the Review of Scientific Instruments 49, (6), June 1978.

19. KEY WORDS (Continue on reverse side if necessary and identify by block number)

High-field permanent magnets
Wide temperature range magnetometer
Zero to 100 kOe magnetometer
Multimode operation magnetometer

20. ABSTRACT (Continue on reverse side if necessary and identify by block number)

A variable temperature magnetometer was built for use with a high-field superconducting solenoid in a liquid helium environment. Measurements can be made at temperatures ranging from 1.5 to 300 K. Three modes of operation are possible: integrating fluxmeter, ballistic magnetometer, and variable temperature. The probe permits quick, efficient sample exchange.

DD FORM 1 JAN 73 1473 EDITION OF 1 NOV 65 IS OBSOLETE

UNCLASSIFIED
SECURITY CLASSIFICATION OF THIS PAGE (When Data Entered)

CONTENTS

FIGURES

Variable temperature multimode magnetometer

J. J. Winter, F. Rothwarf, H. A. Leupold, and J. T. Breslin

US Army Electronics Technology and Devices Laboratory (ERADCOM), Fort Monmouth, New Jersey 07703

(Received 27 December 1977; in final form, 23 February 1978)

A variable temperature magnetometer was built for use with a superconducting solenoid in a liquid helium environment. Measurements can be made at temperatures ranging from 1.5 to 300 K. Three modes of operation are possible: integrating fluxmeter, ballistic magnetometer, and variable temperature. The probe permits quick, efficient sample exchange.

INTRODUCTION

Over the past few years there has been an increasing need to extend the operating spectra of various military microwave devices to even higher frequencies, sometimes well into the millimeter-wave range. Recent design calculations have shown that if this frequency augmentation is to take place without an objectionable increase of the weight and bulk of device components, it would be necessary to employ permanent magnet materials with energy products and temperature independences considerably superior to those of presently existing materials. In the course of research initiated to produce such materials the need arose for a versatile variable temperature magnetometer. An earlier probe design[1] offered the temperature control required in a small diameter configuration. As pointed out previously,[2] however, the circuitry used with that probe measured the slope of the minor hysteresis loop intersecting the magnetization curve at the applied dc field. Thus, the magnetization could not, in general, be retrieved. Therefore, another method of measuring magnetization was required with an attendant alteration in the sensing coil configuration and housing.

The requirements for a long sample rod, for in-house construction, for avoiding sample motion (which can cause flux line disturbance in superconductors, etc.)[3] and the potential need to make I-V measurements simultaneously with magnetization measurements all contributed to the decision to adapt an integrating magnetometer rather than a vibrating sample technique to our probe.

I. EXPERIMENTAL DETAILS

A. Construction

The apparatus consists of four concentric tubes, A, B, C, and D (Fig. 1). In operation, a long sample rod A is inserted into section B. O-rings housed in cylinder B2 make a vacuum-tight seal with A. Housings B2 and B4 are sealed together via Marmon flange B3. Section B is inserted into C and B5 is sealed at the compression O-ring fitting C1. Section B thermally mates with C when conical copper heat sink B6 slides snugly into copper fitting C7. This, in turn, thermally mates with copper fitting D6 which is immersed in the liquid helium bath. Section C is inserted into vacuum jacket D, and C6 is sealed at the O-ring fitting D1. Relief valves C3 and D3 are inserted in the vacuum–He exchange gas valve stems C2 and D2 as a safety precaution to vent gases inadvertently condensed at lower temperatures.

Chambers D, C, and the upper part of B were constructed from 0.25-mm wall nonmagnetic steel tubing of 2.54, 1.905, 0.9525 cm o.d., respectively. The part of B below the heat sink B6 is constructed of linen Bakelite. Thermal grounding of the leads to the heat sink B6 is accomplished by intimate contact of thick Formvar-insulated feedthrough conductors with the channels drilled in B6 and by wrapping about the recessed ends of the heat sink and the steel tubing. A Kimwipe layer saturated with GE 7031 is recommended as a good thermally conductive yet electrically insulating bond between tubing and leads.

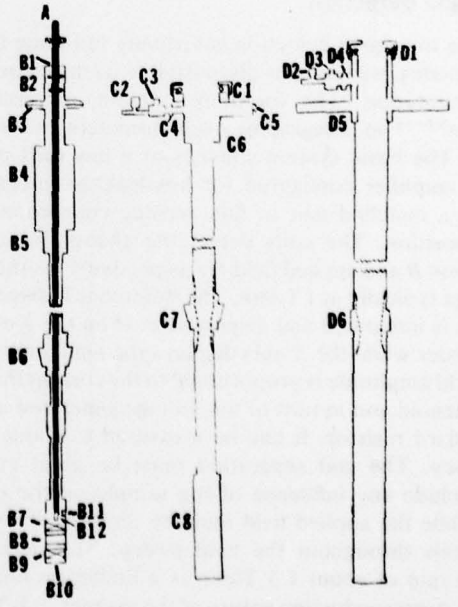

FIG. 1. Variable temperature probe. A—sample rod; B—measurements assembly; C—isothermal chamber; D—vacuum jacket. See text for details.

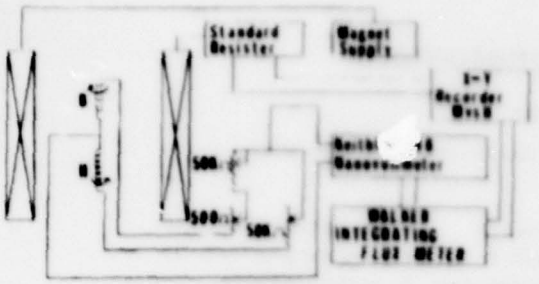

FIG. 2. Schematic diagram of the magnetization detection circuit.

C8 is a copper chamber which houses the pickup coils B7 and B9, the thermometers located at B8 and B11 and the sample B12 which normally resides within B7. Housing B4 contains the hermetically sealed electrical feedthroughs. The pickup coil and thermocouple leads were unbroken[4] up to the analyzing circuitry and the wire itself was chosen because of its homogeneity.[5] A 300-Ω heater is uniformly wrapped around the copper chamber C8 and the heater leads brought out through a slot in C6. This slot was epoxied over after the heater leads were inserted and then machined to permit the vacuum-tight junction of C7 and D1.

The nearly matched 5000-turn pickup coils are 0.635 cm in length and 0.6604 cm i.d., in order to fit the 0.635-cm-diam powder-in-epoxy samples closely, and the coil separation is 3.81 cm to preclude any influence of the sample on the empty field detection coil. These coils are potted with low temperature epoxy, Emerson & Cuming 2651 MM and catalyst 9. Holes in the coil form and support rod permit movement of helium exchange gas throughout the chamber.

B. Signal detection

Since the signal detection is virtually the same for all three modes, we limit our discussion to its most complex implementation. The literature contains several references[3,6–16] to integrating magnetometers of various types. The basic system consists of a low drift operational amplifier configured for low-leakage integration across a matched pair of flux sensing coils connected in opposition. The coils detect the change in sample induction B and applied field H, respectively, as the field is swept typically at 1 T/min. The difference between the signals is integrated and displayed at M on the Y axis of a recorder while the X axis displays the field amplitude. The field amplitude is proportional to the current through the solenoid and in turn to the voltage generated across a standard resistor. It can be measured to about 0.1% accuracy. The coil separation must be great enough to preclude any influence of the sample on the empty coil while the applied field must be uniform across the two coils throughout the field sweep. The maximum sweep rate of about 1.5 T/min is a limitation imposed by the superconducting nature of the magnet. It is below any imposed by the electronics.

The circuit we found convenient is illustrated in Fig. 2. It employs commercial equipment wherever possible. Due to overall system constraints, the simple flux compensation mechanism of Ref. 6, consisting of two nearly identical coils displaced along a common axis, was adopted. See B7 and B9 of Fig. 1. Our circuit diverges from that of Ref. 6, however, in the potentiometer arrangement[17] used to achieve fine balance and in the fact that our signal is amplified before integration. In this latter aspect our circuit becomes similar to that of Refs. 9 and 12–14. As in Refs. 9 and 14, the signal is first amplified by a Keithley 148 nanovoltmeter which has a very low drift rate of 10 nV/day and offers a great range of amplification with high input impedance. We are informed this amplifier generates negligible $1/f$ noise[18] on the millivolt ranges which we employ. As in Ref. 11, our integration is done with an O.S. Walker integrating fluxmeter. The particular model we used was the MF-1R.

While a Hall probe can sometimes[11] be used to good advantage for field detection, a balanced coil system is usually preferred to reduce common mode problems of noise and to approximately cancel thermal emfs. Extensive precautions were taken to avoid thermoelectric effects in wiring the coils, as was noted above. The coils each contained about 5000 turns of #48 copper wire. They were potted with low-temperature epoxy to prevent winding shifts due to both magnetic and thermal cycling.

C. Thermometry

Several different thermometers are deployed in 2 different surface grooves, B8 and B11, of the coil form to monitor thermal gradients as well as temperature. Location B8 houses a 68-Ω, 0.1-W, Allen–Bradley resistor for the range 1.5–20 K, a platinum resistance thermometer[18] for the range 20–300 K, and a field-independent capacitance thermometer[20–22] for the range 1.5–70 K and 90–300 K, which is thermally tied to the other thermometers for mutual comparison. Location B11 houses a copper–Constantan[23] thermocouple for the range 20–300 K and a germanium resistance thermometer[24] for the range 1.5–100 K. We use most of these thermometers at zero field only, but their field dependence has been discussed by Neuringer and Rubin.[25] The field dependence of the carbon thermometer is small, can be readily calibrated, and in part reduced.[26] It is recommended that all potential thermometry requirements be met during initial construction when both the wiring and thermometer placement are simple.

II. OPERATION

A. Integrating magnetometry, varying field, fixed temperature

As field is swept, the change in magnetization with field is integrated and plotted as M vs H (see Sec. I). Signal strength is calibrated by running a nickel sample of the same size and shape. At each substantially different temperature setting (see Sec. III), nanovoltmeter-

fluxmeter drift is zeroed out and coil balance is reestablished by Helipot adjustment while sweeping the field. For this adjustment phase, the sample is conveniently removed from the pickup coil-solenoid region by withdrawal of sample rod A.

B. Integrating magnetometry, varying temperature, fixed field

This mode can be used to study the temperature dependence of the magnetization at fixed fields. Our interests included elucidating such behavior for superconducting materials,[1,2,27] in phase transition regions, and for rare earth–cobalt materials under saturation or zero field conditions. This mode requires determination of the initial magnetization by one of the other modes, most conveniently the ballistic mode. The range of temperature that could be swept per integration would be limited by the necessity for maintaining quasistatic equilibrium. This range would depend on the signal strength, the thermal conductivity and the specific heat of the sample. The change of magnetization is measured as in Sec. I B.

C. Ballistic magnetometry

This mode is used to measure sample magnetization at fixed fields. The signal is generated by abrupt sample removal from the pickup coil and detected as above. Since the coil sensing field-change generates no signal, coil balancing is unnecessary in this mode. The Keithley voltmeter scale is visually monitored during this operation to preclude amplifier saturation. Calibration is as in Sec. II A.

The ballistic mode complements the integration mode in various ways. For example, it may be used to ascertain the state of magnetization of a sample without magnetically altering that state. In addition, high-field magnetometry with our Nb_3Sn magnet is limited to this fixed field measurement due to the relatively long cycling times required to prevent flux jumping at these fields. Martin and Benz[28,29] also employ a ballistic technique with a high-field Nb_3Sn solenoid. Such ballistic measurements and conventional hysteresigraph measurements on saturated samples were made in their study of demagnetization properties of long cylindrical cobalt–rare earth magnets.

D. Temperature control

In our large, slow-cycling, superconducting magnet facility, the probe resides in a chamber that is vacuum isolated from the helium bath of the magnet. Thus temperature control is relatively easy. In our smaller faster cycling system, the probe resides in the helium bath of the magnet and our remarks are directed at this system.

The conically mating copper heat sinks B6, C7, and D6 leak heat to the bath and tend to cool the system while shunting away heat conducted down by the leads and probe structure from room temperature. With a vacuum

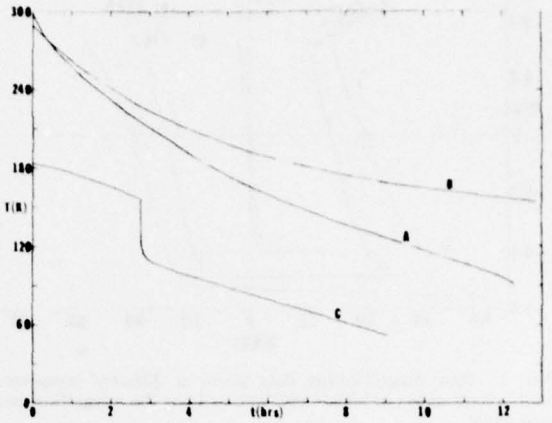

FIG. 3. The cool-down rates of the experimental chamber, C8, for various vacuum chamber (D) pressures. In runs A and B vacuums of 10^{-1} and 10^{-6} Torr, respectively, were established, and the vacuum chamber was sealed before and remained so throughout cool-down. Curve C is effectively a continuation of Curve B but the vacuum chamber valve was opened to a diffusion pump pressure of 10^{-5} Torr at the 1-h mark, then helium gas was injected into the line at the 2:45 mark and reevacuated immediately.

of about 10^{-6} Torr in Chamber D, the equilibrium temperature of the experimental space within copper Chamber C8 is about 25 K. We exercise temperature control of the experimental space by varying the amount of exchange gas in Chamber D and current in the heater wrapped uniformly around Chamber C8.

The utilization of the thermometers described in Sec. I C in achieving temperature control will now be discussed. The Allen–Bradley resistor in location B8 of Fig. 1 and the germanium thermometer in B11 can be monitored to determine temperatures, which are then compared to examine thermal gradients for temperatures below 20 K. The copper–Constantan thermocouple and platinum thermometer are monitored for the temperature range of 20–300 K and the gradients or temperature differences evaluated. The germanium thermometer is useful up to 100 K and is preferred over the thermocouple at the lower temperatures. The resistive devices are measured using a constant current supply and digital voltmeter with a resolution of about 0.1 μV. Currents of 10 μA or less are generally required to avoid heating. Magnetization measurements are not performed until the temperature is sufficiently stabilized.

The application of field affects the accuracy of the above thermometers and with the exception of the Allen-Bradley resistor they can be monitored only before and after field excursions. The capacitance thermometer is field independent and is monitored with a General Radio 1615A capacitance bridge when required. It is most conveniently employed as a null detector to indicate little or no change in temperature during a field excursion.

Figure 3 illustrates how cool-down varies as a function of the vacuum pressure in Chamber D. Curves A and B were obtained by pulling vacuums of 10^{-1} and 10^{-6} Torr, respectively, valving off the vacuum system

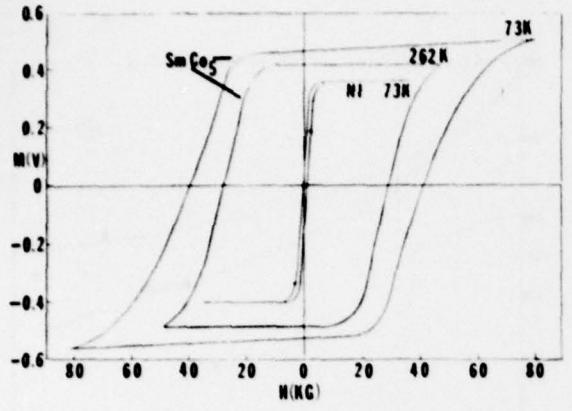

FIG. 4. Raw magnetization data taken at different temperatures on 0.318-cm cubes of nickel and $SmCo_5$ using the integration-swept-field mode.

and then lowering the magnetometer assembly into the liquid helium bath. Curve C is effectively a continuation of Curve B.

If integrating fluxmeter measurements are to be made on a single sample at different temperatures, the cool-down rate of Curve B is slow enough to introduce no detectable error in the typical hysteresis loop. In this regard a brief analysis of ΔM, the error in magnetization resulting from the thermal drift is worth consideration.

$$\Delta M = \int_0^{t_L} \frac{dM}{dT}\frac{dT}{dt}\,dt,$$

where dM/dT is the rate of change of magnetization with temperature, dT/dt is the rate of change of temperature with time, and t_L is the time required to trace a loop, 10–20 min. Figure 4 illustrates the typical change in magnetization, for $SmCo_5$ roughly 10%, for temperature changes from 273 to 77 K. Approximating dM/dT then by $(M_s/10)/200$ K, where M_s is the saturation magnetization, and estimating dT/dt at 273 K, from curve B of Fig. 3, to be 6 K/13 min and assuming a period, t_L, to be 13 min we obtain $\Delta M \approx 0.003\ M_s$. Thus ΔM is well below the resolution of the $M-H$ curves shown in Fig. 4.

If room temperature measurements are to be made on a number of samples, stabilization becomes necessary. The temperature can be stabilized at 300 K by application of about 1 W of power when a pressure of 10^{-6} Torr has been established in the vacuum chamber before valving off and before submersion in liquid helium.

Measurements made at 4.2 K require helium exchange gas in Chambers D and C. Typically we use about 10 cm^3 aliquots of helium gas at 300 K and 150 Torr in Chambers D and C, which each have volumes of about 300 cm^3, to equilibrate the probe temperature with that of the helium bath.

E. Sample change

To remove sample rod A, Chamber D must be evacuated to more effectively isolate Chamber C from the liquid helium bath. Then we apply an overpressure of helium gas at C2 to reduce air intake at orifice B1 when A is fully removed for sample change. B1 is then plugged while the sample holder is replaced. The samples are glued to threaded sample holders with GE 7031. Rod A is reinserted under the same overpressure of helium gas then Chamber C is evacuated, purged with helium gas, and reevacuated.

III. MEASUREMENT AND ANALYSIS

Maximum sensitivity is attained with samples that fit the pickup coil closely and have a high density of active material. All our samples met at least one of these criteria.

Cylindrical samples composed of 5% suspension of $Sm_2(CoFeMn)_{17}$ alloy in epoxy were designed with a diameter of 0.627 cm. The i.d. of the pickup coils is 0.66 cm. Although a sample length of 0.7 would have optimized detection a length of 0.35 was chosen to meet the constraints of another system. The results of measurements on these samples will be published elsewhere.[30] These sample runs, in general, required cycle times of twenty minutes to attain fields of ±85 kG. Practical resolution was limited by drift to about 10 G. Scale factors of 1 mV on the nanovoltmeter and 50.00×10^4 on the fluxmeter produced displacement ratios of about ¼ mm/G on the recorder. Thus a visual resolution of about 1 G is possible. This is about 1/10 the drift uncertainty. Improved resolution depends only on reducing the drift rate.

Solid $SmCo_5$ cubes of only 0.32 cm on a side were also measured. Figure 4 illustrates curves obtained from these cubes at different temperatures. The results from a nickel cube are also displayed for comparison. The scale factors employed for these measurements were 3 mV on the nanovoltmeter and 50.00×10^4 on the fluxmeter.

Demagnetization effects of nonelliptical specimens can be complex and must in general be resolved.[8,28] When the principal aim is determination of the anisotropy field of a cylinder, analysis is simplified. Anisotropy is determined by applying an axial field on cylindrical samples whose crystallites are aligned with their easy axis in the direction of a diameter. The applied field at which saturation occurs is then the sum of the anisotropy field and the demagnetization field in a particle at the center of the cylinder because the center is where the total field is smallest and hence the last part of the sample to saturate. Thus to determine H_A one need only find the field in a particle at the center of an axially saturated cylinder in an applied field $H_A{}^0$. H_A is then given by

$$H_A = H_A{}^0 - H_D{}^C + H_D{}^E - H_D{}^P, \qquad (1)$$

where $H_D{}^C$, $H_D{}^E$, and $H_D{}^P$ are demagnetization fields arising from magnetic poles located, respectively, on the ends of the cylinder, on the epoxy side of the boundary between the particle and the epoxy, and on the

particle side of the epoxy–particle boundary. H_A'' is given by the familiar expression for the field halfway along the axis of two equally and uniformly but oppositely charged circular laminae.

$$H_A'' = 4\pi SM_s[1 - (1 + r^2)^{-1/2}] \qquad (2)$$

where S is the ratio of powder to sample volume, r is the sample diameter to length ratio, and M_s is the saturation magnetization. If one assumes an average spherical shape for the powder particles,

$$H_D^E = 4\pi SM_s/3 \qquad (3)$$

$$H_D^P = 4\pi M_s/3. \qquad (4)$$

Substituting Eqs. (2)–(4) in (1) then yields

$$H_A = H_A'' - 4\pi SM_s[\tfrac{2}{3} + \tfrac{1}{3}S - (1 + r^2)^{-1/2}] \qquad (5)$$

For homogeneous magnetic samples, terms (3) and (4) do not exist and (5) reduces to

$$H_A = H_A'' - 4\pi SM_s[1 - (1 + r^2)^{-1/2}]$$

The results from a $Sm_2(Co_{0.6}Fe_{0.4})_{17}$ powder-in-epoxy cylinder of diameter 0.426 cm and length 0.42 cm are considered as an example. The applied field at saturation was measured to be 85.6 kG and the correction was calculated to be 5.1 kG; thus the anisotropy field is determined to be 80.5 kG.

ACKNOWLEDGMENT

We would like to express our appreciation to Leslie Wilcox for his fabrication of the probe and for his ingenuity in solving many of the construction problems.

[1] F. Rothwarf, D. Ford, and L. W. Dubeck, Rev. Sci. Instrum. **43**, 317 (1972).
[2] H. A. Leupold, F. Rothwarf, J. J. Winter, J. T. Breslin, R. L. Ross, T. R. AuCoin, and L. W. Dubeck, J. Appl. Phys. **45**, 5399 (1973).
[3] P. R. Brankin, J. Phys. E, **3**, 312 (1970). This and other problems with vibrating sample magnetometry are mentioned.
[4] The prescription for reducing thermals is to avoid junctions; if unavoidable, use only pure copper wire and crimps. If solder must be used, make it CdSn and mount all non-copper junctions to a common thermal mass. The Keithley low thermal connection kit 1483 is a convenient form in which to purchase these items.
[5] L. L. Sparks and R. L. Powell, ASTM Standards, Aug. (1971).
[6] W. A. Fietz, Rev. Sci. Instrum. **36**, 1621 (1965).
[7] A. D. McInturf, J. Appl. Phys. **40**, 2431 (1969).
[8] H. Fay, Rev. Sci. Instrum. **43**, 1274 (1972).
[9] H. Brechna, M. A. Allen, and J. K. Cobb, J. Appl. Phys. **42**, 103 (1971).
[10] E. T. Powner, J. B. McKinnon, and P. J. Elce, Electron. Eng. **42**, 52 (1970).
[11] D. Das, A. Gale, and D. Joaquin, Tech Rpt. Pt-3051, AFML-TR-151, p. 28.
[12] C. S. Furtado, Cryogenics **13**, 639 (1973).
[13] C. H. Haakana *et al.*, J. Appl. Phys. **34**, 1178 (1963).
[14] P. Mazzetti and P. Soardo, Rev. Sci. Instrum. **37**, 548 (1966).
[15] H. J. Oguey, Rev. Sci. Instrum. **31**, 701 (1960).
[16] R. Scholes, IEEE Trans. Mag. **MAG-6**, 289 (1970).
[17] The arrangement we use permits potentiometric coil balancing without incurring current flow through one of the pickup coils and the unbalanced emf, $L(dI/dt)$, which results. As Feitz[6] shows, this is, in general, not a serious problem and its effects can be calculated and reduced, perhaps to negligible proportions. Some researchers[7,10] avoid the problem by matching the sensitivities of the coils themselves but this requires repeated testing and rewinding.
[18] We are told by the designer of the Keithley 148 nanovoltmeter that the only significant $1/f$ noise generated is that due to the leads and connectors and this is taken out by the chopper circuit in the front end which operates at 94 Hz. He asserts that $1/f$ noise should be of no concern particularly at the scale sensitivities we employ, 1–10 mV. Oguey in his report on an ultrasensitive magnetometer for measurement of thin magnetic films[15] cautions the reader about generating $1/f$ noise in an amplifier stage before integration. For tube amplifiers he recommends that the pickup coils have the maximum number of turns possible to swamp out the $1/f$ noise. The nanovoltmeter we used was purchased in 1965 and we understand it does not have the FET input used in the later models. The first two amplifier stages are tube amplifiers. The pickup coils we employed were maximized within our overall system constraints and contain 5000 turns. We do not in fact see the large slow vertical displacement of the M–H pattern on the X–Y recorder that Oguey predicts will develop with integration of significant $1/f$ noise. The reader should consult Oguey for further discussion of $1/f$ noise and its reduction.
[19] Minco Products, Inc., 7300 Commerce Lane, Minneapolis, MN, 55432. The S1055, S1059, and S1061 models are recommended.
[20] Lake Shore Cyrotronics, Inc., P.O. Box 29876 Columbus, OH 43229.
[21] W. N. Lawless, Rev. Sci. Instrum. **42**, 561 (1971).
[22] L. G. Rubin and W. N. Lawless, Rev. Sci. Instrum. **42**, 571 (1971).
[23] We had originally installed a gold-iron vs Chromel P thermocouple for studies in the range 1.5–77 K. This developed a break. Subsequent replacement was with a copper–Constantan thermocouple which was then useful for the range 20–300 K. Better choices perhaps exist but were not available at the time.
[24] Scientific Instruments, 632 South "F" St., Lake Worth, FL 33460.
[25] L. J. Neuringer and L. G. Rubin, *Temperature* (Instrument Society of America, 1977), Vol. 4, p. 1085.
[26] W. F. Schlosser and R. H. Munnings, Cryogenics **12**, 225 (1972).
[27] F. Rothwarf, J. A. Schmitz, C. C. Dickson, R. C. Thiel, H. Boller, and E. Parthe, Phys. Rev. **152**, 341 (1966).
[28] D. Luther Martin and M. G. Benz, IEEE Trans. Magn. **MAG-8**, 35 (1972).
[29] M. G. Benz and D. L. Martin, GE Rpt. #70-C-318, Sept. 1970, G.E. Research and Development Center, Schenectady, NY. Presented at IEEE Conference Electron Device Techniques, September 1970, New York, NY.
[30] H. A. Leupold, F. Rothwarf, J. J. Winter, J. T. Breslin, A. Tauber, and A. Schwartz, *Proceedings of the 2nd International Symposium on Coercivity and Anisotropy of Rare Earth-Transition Metal Alloys*, University of California, San Diego, July 1, 1978.